

CLNS 01/1765
October 17, 2001

CKM Status and Prospects

Brian K. Heltsley

Laboratory of Nuclear Studies, Cornell University, Ithaca, NY 14853

*To appear in the proceedings of the
XXI Physics in Collision Conference
Seoul, Korea, 28-30 June, 2001*

ABSTRACT

This presentation reviews the Standard Model formalism governing the weak decays of quarks, as embodied in the Cabibbo-Kobayashi-Maskawa (CKM) weak mixing matrix, and summarizes the experimental status and outlook. Two recent CLEO $|V_{cb}|$ analyses are described. Complications from strong interactions in relating the experimentally accessible quantities to CKM elements are highlighted, and prospects for addressing those difficulties with LQCD and CLEO-c are outlined.

1 Introduction

We gather at an auspicious time for particle physics in general, and heavy flavor physics in particular. The highly successful LEP program has concluded, making way for the LHC. Run II at the Tevatron is underway. Efforts to

complete the B -factories and harvest their results have nearly come to fruition: KEK-B and PEP-II have achieved luminosity exceeding expectations, and Belle and BaBar both presented initial results last summer. It is widely anticipated that, in the coming weeks, direct and definitive measurements of non-zero CP violation in the B -meson system will be announced by one or both B -factory collaborations. Such a development would undoubtedly intensify the spotlight on the heavy quark sector of the Standard Model.

Just two days prior to the opening of this conference, the CESR/CLEO B -physics program concluded two decades of data-taking, marking a shift of their focus from B 's to D 's, ψ 's, and Υ 's. This shift is embodied in the imminent CESR-c/CLEO-c project, which will have unique capabilities to pursue precision charm measurements and QCD tests that are essential to our understanding of the heavy flavor sector.

Activity and broad interest in the weak decays of heavy quarks and related issues has never been higher. The landscape is changing rapidly. This review provides a snapshot of that landscape as of early summer 2001.

2 CKM, the Unitarity Triangle, and CP Violation

In the Standard Model, the charged current weak interactions of three generations of quarks are governed by a Lagrangian which contains a transformation from the mass eigenbasis to the flavor (generation) eigenbasis.^{1, 2, 3} This flavor-mixing is expressed as a 3×3 complex matrix V known as the Cabibbo-Kobayashi-Maskawa (CKM) matrix.^{4, 5} The elements V_{ij} determine the relative weak couplings of the charge $-\frac{2}{3}$ quarks $i = (u, c, t)$, one row each, to the charge $+\frac{1}{3}$ quarks ($j = d, s, b$), one column each. By definition, the matrix V is **unitary**. Unitarity reduces the number of independent parameters to nine, which can be chosen as three real mixing angles and six imaginary phases. Five of the phases are removable. The four remaining parameters are fundamental constants of nature to be determined by experiment; the Standard Model itself gives no guidance as to their values.

The successive application of charge conjugation (C), parity reversal (P), and time reversal (T) is an exact symmetry of any local Lagrangian field theory. The electromagnetic and strong interactions preserve all three symmetries separately; weak interactions violate C and P separately but together appear to preserve CP with the exception of neutral kaon (and perhaps beauty) de-

cays. Within the Standard Model framework, CP violation can occur only if the one irremovable CKM phase is non-zero. CP violation would not happen, however, if any two same-charge quarks have equal masses, if any mixing angle is 0 or $\frac{\pi}{2}$, or if the sine of the phase is zero.

It is instructive to note a couple of special cases: first, if applied to the leptonic sector, in the limit of vanishing neutrino masses, the mixing matrix is trivially the identity (i.e. no mixing and no CP -violation); second, the unitarity constraint in the case of just two quark generations leaves no irremovable phase and hence no CP violation. The latter property of V and the existence of CP violation in neutral kaon decay provoked the hypothesis of a third generation⁵⁾ before its experimental discovery. With such a history, it is not surprising that experimental unitarity tests continue to be pursued vigorously.

The unitarity constraint imposes unity normalization on all rows and columns as well as their orthogonality. The orthogonality relations can be described geometrically by six “unitarity triangles” in the complex plane: each side of the jk triangle is a vector $V_{ij}V_{ik}^*$. All six triangles have the same area, which is non-zero only if CP violation occurs.

With the $\sim 1\%$ knowledge from experiment of $|V_{cd}| \approx |V_{us}| = \lambda \equiv \sin \theta_C = 0.22$, it can be shown that four of the unitarity triangles (ds , sb , uc , ct) have one side that is smaller by two or more powers of λ than the other two sides. The db and ut triangles have three comparable sides of length $\sim \lambda^3$. The db triangle, also known as *the* Unitarity Triangle (UT), is described by

$$V_{ud}V_{ub}^* + V_{cd}V_{cb}^* + V_{td}V_{tb}^* = 0. \quad (1)$$

By convention, $V_{cb}^*V_{cd}$ is used to normalize the other UT sides, forming the *rescaled* UT shown in Fig. 1. Of the six triangles, the one described by Eq. 1 has attracted the most attention due to the relative accessibility of sides and angles to experiment. Several measurements can be used in combination to directly test unitarity, and hence the validity of the Standard Model itself.

One favored explicitly unitary parameterization of V has three mixing angles and a phase.¹⁾ Generational symmetry and therefore ease of interpretation are preserved in this representation. However, currently prevalent is the Wolfenstein⁶⁾ formulation as modified by Buras⁷⁾

$$V = \begin{pmatrix} 1 - \frac{\lambda^2}{2} & \lambda & A\lambda^3(\rho - i\eta) \\ -\lambda - iA^2\lambda^5\eta & 1 - \frac{\lambda^2}{2} & A\lambda^2 \\ A\lambda^3(1 - \bar{\rho} - i\bar{\eta}) & -A\lambda^2 - iA\lambda^4\eta & 1 \end{pmatrix} \quad (2)$$

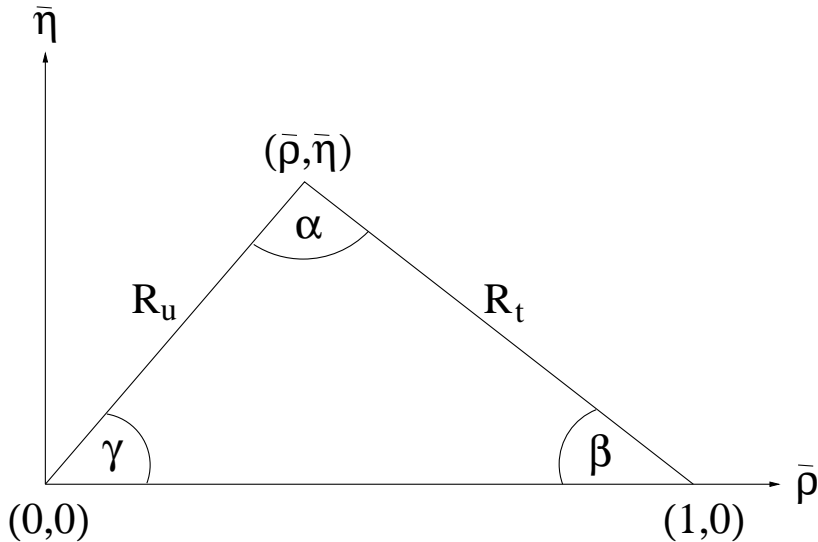


Figure 1: *The rescaled Unitarity Triangle in the Wolfenstein-Buras formulation, in which $R_x = |V_{xd}V_{xb}^*/(V_{cd}V_{cb}^*)|$. [from ref. 8]*

in which $\lambda \equiv \sin\theta_C \approx 0.22$ has become an expansion parameter, and terms of order λ^6 ($\sim 10^{-4}$) and higher are dropped. The Buras corrections, addition of the terms of higher order than λ^3 and the rescaling of ρ and η in V_{td} to $\bar{\rho} \equiv \rho(1 - \frac{\lambda^2}{2})$ and $\bar{\eta} \equiv \eta(1 - \frac{\lambda^2}{2})$, attain better precision and exact unitarity. The four fundamental couplings are then λ , A , $\bar{\rho}$, and $\bar{\eta}$. Here the rescaled UT has vertices in the complex plane at $(0,0)$, $(1,0)$, and $(\bar{\rho}, \bar{\eta})$ as in Fig. 1. The attraction of this representation is that the hierarchy of matrix element sizes in powers of λ is explicit, as is the presence of the UT coordinates $(\bar{\rho}, \bar{\eta})$ as separate fundamental constants. The internal angles β , γ , and α (or ϕ_1 , ϕ_3 , ϕ_2 , respectively) can be taken as an alternative basis for CKM parameters.⁹⁾

CP violation occurs only if $\bar{\eta}$ (and therefore β) are non-zero. Within the Standard Model framework, measurement of CP -conserving decays can determine the lengths of the UT sides, and therefore *indirectly* the value of a non-zero CP -violating β . However, the three individual angles and their sum must all be subjected to measurement for consistency with unitarity to test the limitations of the Standard Model itself. Eventually, all the unitarity triangles

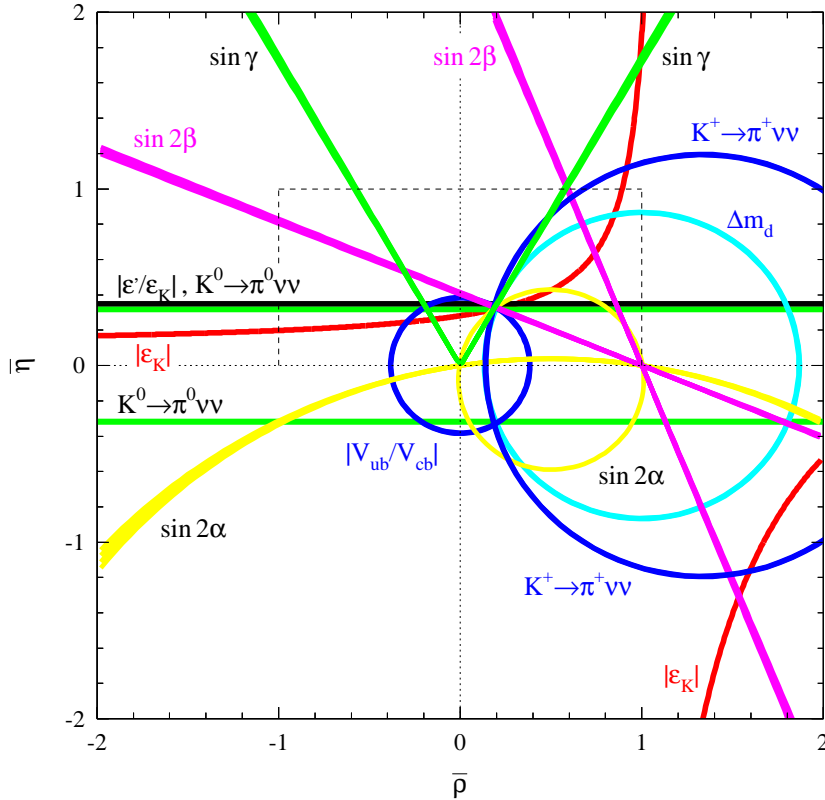


Figure 2: *Contours in the $\bar{\rho}, \bar{\eta}$ plane corresponding to hypothetical precision measurements of nine observables, arranged to be consistent with unitarity by overlapping at a fixed (arbitrary) point $\sim (0.2, 0.35)$. [from ref. 8]*

need to be probed for consistency among sides and angles; some will be easier and/or cleaner than others.

Global fitting can improve the metrological accuracy of all the CKM couplings. Fig. 2 shows the contours that would result from hypothetical precision measurements of nine observables, the values of which were chosen to be consistent with unitarity and therefore all intersect at a point. The reality now is that only a few of those quantities have been determined at all, and, for the most part, not very precisely.

3 Complications from Strong Interactions

Because hadrons, not quarks, are produced and observed in the laboratory, CKM matrix elements generally cannot be extracted from experiment without understanding the effects of strong interactions on the initial and/or final state particles. The required computational alacrity must come from quantum chromodynamics (QCD), the gauge theory of quarks and gluons. Although modeled after QED, QCD differs in the non-linearity of its field equations (because gluons carry color charge), and the permanent confinement of quarks inside hadrons (due to strong coupling). Asymptotic freedom has allowed the development of perturbative QCD, which has been very successful in describing high momentum-transfer (QED-like) processes such as deep inelastic scattering (DIS) and high energy quark and gluon jets. However, untangling CKM matrix elements from the weak interactions of hadrons frequently requires theoretical understanding of the low energy, non-perturbative regime. Such understanding can be described presently as incomplete at best.

Lattice QCD (LQCD), Heavy Quark Effective Theory (HQET), the Operator Product Expansion (OPE), and several models all currently enjoy varying degrees of success in calculating effects of strong interactions. HQET predictions are rigorously accurate in the limit of infinitely heavy quark masses, and hence must be corrected in powers of $1/M_q$. Models are generally tuned to reproduce one set of observations and then applied to predict others. LQCD, however, is a complete definition of the theory. Although unproductive for most of its existence, LQCD has recently overcome technical problems¹⁰⁾ and adopted new algorithms¹¹⁾ which, along with availability of inexpensive computing power, offer the hope of $\sim 1\%$ precision on dozens of quantities within the next five years. Already some form factors, decay constants, and glueball masses have LQCD predictions estimated to be accurate at the 10-15% level.

Quantities needed from non-perturbative QCD include decay constants, form-factors, and bag parameters. The decay constant appears in the leptonic decay of a meson Q as $\mathcal{B}(Q \rightarrow l\nu) \sim m_l^2 f_Q^2 |V_{qj}|^2 \tau_Q$. Unfortunately such branching ratios of D 's and B 's are small enough to make purely leptonic decays not useful at present. Form-factors $F_X(q^2)$ play an analogous role in the q^2 -dependence of semi-leptonic decays $d\Gamma/dq^2(Q \rightarrow Xl\nu) \sim p_X^3 |V_{qj}|^2 |F_X(q^2)|^2$ and are specific to the hadronic final state X . The q^2 dependence is helpful independently from the overall normalization because the form-factor value at

zero recoil ($q^2=0$) is accessible to HQET; one can extrapolate the measured $F(q^2)|V_{qj}|$ to $q^2 = 0$ to extract $|V_{qj}|$. The bag parameter appears with the decay constant squared in $f_Q^2 \hat{B}_Q |V_{tj}|^2$, the expression for the frequency (neutral meson mass difference) of $Q \iff \bar{Q}$ oscillations (i.e. K^0 , B_d and B_s mixing), which are dominated for B 's by box diagrams with t and W sides.

Inclusive measurements of semi-leptonic decays of charm and bottom are employed to avoid the need for form-factors, relying on HQET for the necessary quark-level input. These results rest upon the assumption of *quark-hadron duality*, which presumes that integrated over a broad enough spectrum of hadronic final states and phase space, the measured quantity is the same as the quark-level prediction. Some take this duality as a given, especially for unrestrictive event selections; some express reservations and wonder how to assess uncertainties when experimental cuts are quite narrow, and some take inclusive results as measurements not of CKM parameters but of the validity of the duality assumption itself. In any case, inclusive measurements can be instructive as to the underlying physics and assumptions.

4 CKM Status without Unitarity

What do we know about the CKM elements now, without unitarity constraints? Of the nine absolute values, two are measured to $\leq 1\%$, three more are known to $\sim 6\%$, and the remaining four are uncertain at the $\geq 15\%$ level. Measurements of super-allowed and neutron β -decays ^{1, 12)} yield $|V_{ud}| \approx 0.974 \pm 0.001$. Analysis ^{1, 13)} of neutral and charged K_{e3} decays ($K \rightarrow \pi e \nu$) yields $|V_{us}| \approx 0.2196 \pm 0.0023$, which is verified by a somewhat less precise result from hyperon semi-leptonic decays. ¹⁴⁾ Di-muon production in DIS of ν and $\bar{\nu}$ on nucleons, one muon from a semi-leptonic charm decay, has been examined ¹⁵⁾, yielding $|V_{cd}| = 0.224 \pm 0.016$ and $|V_{cs}| = 1.04 \pm 0.16$. From direct production of charm in real W decays, ¹⁶⁾ $|V_{cs}| = 0.969 \pm 0.058$, considerably more accurate than DIS. $|V_{cs}|$ from $D \rightarrow K e \nu$ decays ¹⁾ is consistent but has an error nearly three times larger, due mostly to uncertainty in the form-factor. Measurements of the b -fraction in top quark decays by CDF and D0 result in the rather loose restriction ¹⁾ of $|V_{tb}| < (0.99 \pm 0.15) \times U_t$ where $U_t^2 = \sum_j |V_{tj}|^2$.

The remaining CKM elements (third row and column) can be measured with B -decays. Currently there is information from both inclusive and exclusive semi-leptonic decay branching ratios for V_{ub} and V_{cb} . The heavy-to-heavy

transition in inclusive $b \rightarrow c l \nu$ is more easily calculable in HQET than for $b \rightarrow u l \nu$; the published numbers are $|V_{cb}| = (40.7 \pm 0.5 \pm 2.0) \times 10^{-3}$ from LEP ¹⁷⁾ and $|V_{cb}| = (41 \pm 2 \pm 2) \times 10^{-3}$ from CLEO, ¹⁸⁾ in which the errors are experimental and theoretical, respectively. Both are subject to the inherent assumption of quark-hadron duality. Exclusive results from LEP and CLEO for $|V_{cb}|$ also give results in this range, as seen in Section 5.

$|V_{ub}|$ is difficult due to the enormous charm background over all but the lepton-momentum spectrum's endpoint region, and the difficulty of obtaining the requisite QCD information to extract it from the branching fraction. Two different strategies have emerged. The inclusive LEP analysis includes a wide kinematic range to avoid losing signal statistics but then pays the price of quark-hadron duality and a fine-tuned modeling of charm backgrounds. CLEO restricts itself to exclusive final states ($B \rightarrow \pi l \nu, \rho l \nu$) using ν -reconstruction, in which there is a more favorable signal-to-noise but a considerable uncertainty in the form-factors. The LEP value ¹⁹⁾ $|V_{ub}| = (4.09^{+0.59}_{-0.69}) \times 10^{-3}$, in which experimental and modeling errors make comparable contributions, is consistent with that from CLEO, ²⁰⁾ $(3.25 \pm 0.30 \pm 0.55) \times 10^{-3}$, in which the first error is experimental and the second is theoretical.

Measurement of the frequency of oscillations in the B_d and B_s systems yields ²¹⁾ $\Delta m_d = 0.489 \pm 0.008 \text{ ps}^{-1}$ and $\Delta m_s > 14.6 \text{ ps}^{-1}$. Relating these to the CKM matrix elements requires knowing $\hat{B}_x f_{B_x}^2$ for each meson. In the case of B_d it can be computed using LQCD to within $\sim 20\%$, yielding $|V_{tb}^* V_{td}| = (8.3 \pm 1.6) \times 10^{-3}$. The ratio $\Delta m_s / \Delta m_d$ is more tractable theoretically than Δm_s alone due to the cancelation of several factors as well as the feature that only the ratio of bag parameters comes into play, not their absolute values. LQCD has given $\sim 10\%$ errors in the ratio $\xi^2 = \hat{B}_d f_{B_d}^2 / (\hat{B}_s f_{B_s}^2)$, translating the Δm_s limitation to $|V_{td}| < 0.24 |V_{ts}|$.

Two measurements of CP -violation put limits on CKM matrix elements. The relationship of the CP -violating parameter ϵ_K in neutral kaon decay to CKM elements is limited not by experiment but by uncertainty in the bag constant B_K which currently has a $\sim 15\%$ uncertainty. In contrast, the UT angle $\beta \equiv \arg(-V_{cd} V_{cb}^* / (V_{td} V_{tb}^*))$ is directly sensitive to the magnitude of the asymmetry between mixed and unmixed neutral B_d decays to the same color-suppressed CP eigenstate, suffering only very small theoretical uncertainties. This explains why it is the first and foremost target of the B -factories. ²²⁾

Although the world average of $\sin 2\beta = 0.48 \pm 0.16$ is three standard deviations from zero, it may be prudent to exercise some caution in regarding this as observation of CP violation, because no single experiment as yet has a two-standard deviation effect. However, with almost no theoretical uncertainty and systematic errors at the ± 0.05 level or better, both Belle and BaBar have the data in hand for such unambiguous discovery.

5 New CLEO Results on $|V_{cb}|$ from $D^*l\nu$ and Moments

CLEO has a new preliminary analysis of $B \rightarrow D^*l\nu$ using both D^{*+} and D^{*0} . Both signal and $D^*Xl\nu$ backgrounds are determined by fitting data distributions in a kinematic variable sensitive to their relative contributions. These fits are performed in bins of a q^2 -substitute HQET variable w , which is the D^* boost in the B rest frame and has range $1 < w < 1.5$. The fits in a sample w -bin and the overall resulting raw w -distributions are shown in Fig. 3. The efficiency-corrected $F(w)|V_{cb}|$ distribution appears in Fig. 4. Both CLEO and LEP extrapolate to the HQET-friendly, zero-recoil value $w=1$ with the same functional form. The w -curvature parameter is ρ^2 (not to be confused with the CKM parameter ρ). The CLEO [LEP] ¹⁷⁾ results are $F(1)|V_{cb}| = (42.2 \pm 1.3 \pm 1.8) [(35.6 \pm 1.7)] \times 10^{-3}$ and $\rho^2 = 1.61 \pm 0.09 [1.38 \pm 0.27]$. CLEO finds *both* a smaller $D^*Xl\nu$ background than LEP, which instead of fitting the data for background uses a fixed value from a tuned model, ²³⁾ and a larger curvature ρ^2 . These variables are correlated in the final result, as shown in Fig. 4. The LEP and CLEO results are marginally consistent. Care should be taken in directly comparing $|V_{cb}|$'s quoted from these analyses, as the LEP WG uses ^{17, 24)} $F(1) = 0.88 \pm 0.05$ and CLEO prefers 0.913 ± 0.042 . The CLEO value is more central to the range of predictions, which have a $\sim 5\%$ spread. Using these $F(1)$'s makes the $|V_{cb}|$'s seem closer than they actually are.

CLEO has released an interesting new result ²⁵⁾ for $|V_{cb}|$ based on the combination of an inclusive $b \rightarrow cl\nu$ analysis and the distributions in two seemingly unconnected variables, the γ energy in $b \rightarrow s\gamma$ and the hadronic mass-squared in $B \rightarrow Xl\nu$. The connection is made by HQET, which predicts ²⁶⁾ the form of the function $h(\bar{\Lambda}, \lambda_1)$ in $|V_{cb}|^2 = \Gamma(b \rightarrow cl\nu) \times h(\bar{\Lambda}, \lambda_1)$, in which $\bar{\Lambda}$ represents the mass of light quark and gluon degrees of freedom and $-\lambda_1$ the average momentum-squared of the b -quark inside the B -meson. These parameters, in turn, can be determined from the first moments $\langle E_\gamma \rangle$

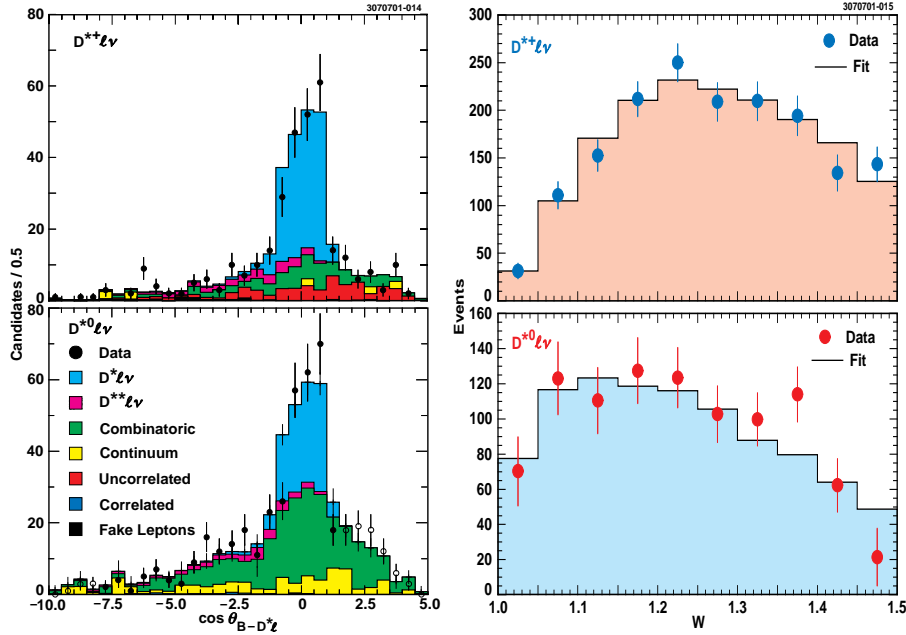


Figure 3: Distributions from the preliminary CLEO analysis of $B \rightarrow D^* l \nu$, in the kinematic variable (left) used to distinguish among and fit signal and various background contributions in a particular w -bin (1.10 – 1.15); on the right the event yields are shown as a function of w along with the fit of Fig. 4.

in $b \rightarrow s \gamma$ (sensitive to $\bar{\Lambda}$ only) and $\langle M_X^2 - \bar{M}_D^2 \rangle$ in $B \rightarrow X l \nu$, where \bar{M}_D is the spin-averaged D -mass, $\bar{M}_D = 0.25M_D + 0.75M_{D^*}$ (sensitive to both $\bar{\Lambda}$ and λ_1). The relevant experimental distributions are shown in Fig. 5. The relation of these values to the HQET parameters is shown in Fig. 6; the values at the intersection of the bands are then inserted into $h(\bar{\Lambda}, \lambda_1)$. The result is $|V_{cb}| = (40.4 \pm 0.9 \pm 0.5 \pm 0.8) \times 10^{-3}$, with the errors covering uncertainties due to experimental determination of Γ , experimental determination of $(\bar{\Lambda}, \lambda_1)$, and the theoretical accuracy for h ($1/M_B^3$ terms and scale α_s), in that order. This result is subject to usual quark-hadron duality caveats associated with inclusive analyses. 27)

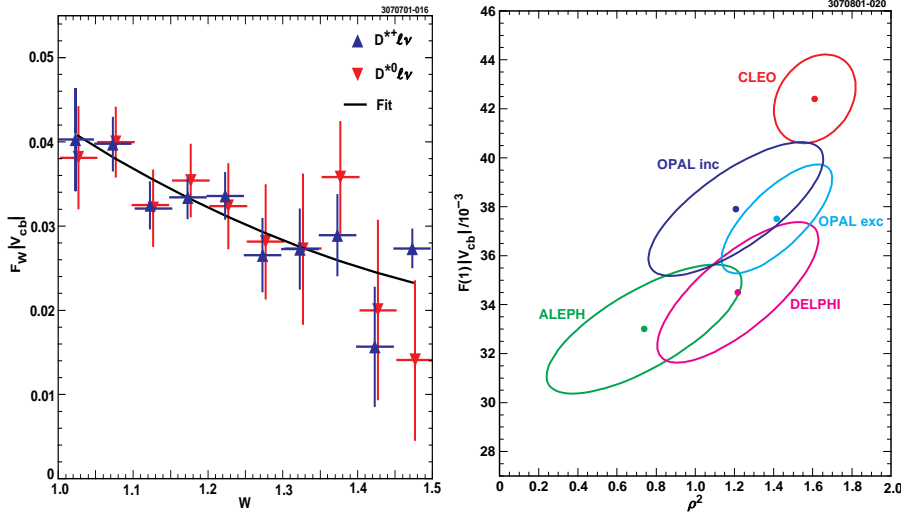


Figure 4: Left: $F(w)|V_{cb}|$ from the preliminary CLEO $B \rightarrow D^* \ell \nu$ analysis and resulting fit. Right: $\Delta\chi^2 = 1$ contours in the ρ^2 - $F(1)|V_{cb}|$ plane for the OPAL, DELPHI, ALEPH, and preliminary CLEO $b \rightarrow c$ analyses.

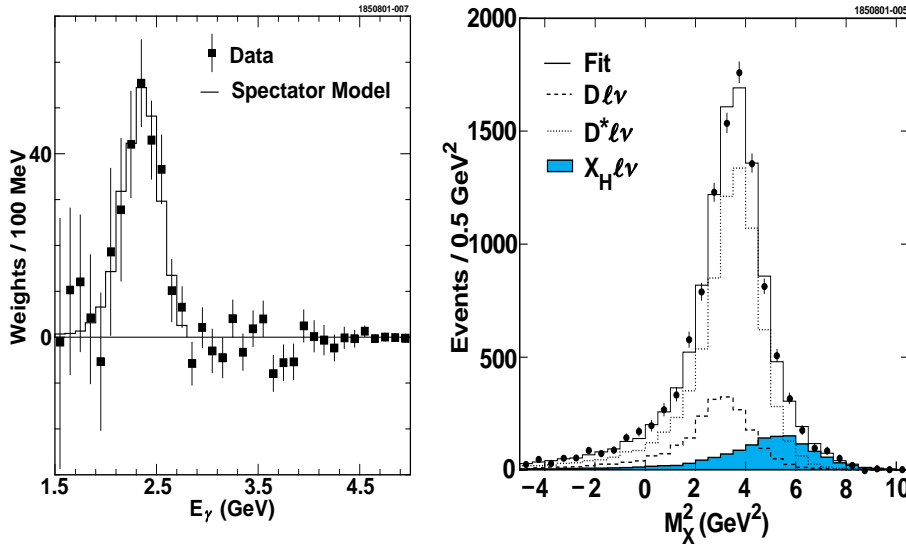


Figure 5: Distributions used as input to the preliminary CLEO “moments” analysis for V_{cb} from inclusive $b \rightarrow c\ell\nu$; on the left E_γ is shown for CLEO $b \rightarrow s\gamma$ data along with a Monte Carlo prediction from a tuned spectator model, and on the right the hadronic mass for CLEO $B \rightarrow X_c \ell \nu$ events.

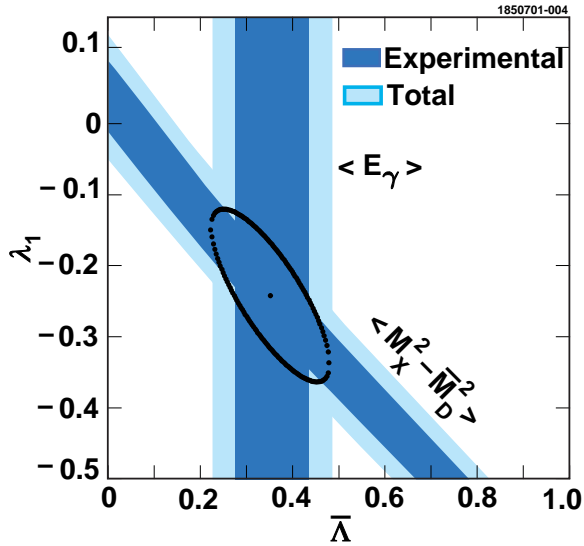


Figure 6: 68% confidence level bands in the $(\bar{\Lambda}, \lambda_1)$ plane from the preliminary CLEO measurements of the first moments of the distributions in Fig. 5. The narrower bands include only experimental errors and the wider ones include $\sim 1/M_B^3$ theoretical uncertainty estimates.

6 Imposing Unitarity with Global Fits

Fig. 7 shows the allowed bands in the $(\bar{\rho}, \bar{\eta})$ -plane from four of the measured quantities. Their overlap or lack thereof is a measure of consistency with the Standard Model, and they can be combined to extract “best-fit” results for all the CKM-related quantities. The experimental and theoretical inputs themselves can be floated in the fits as well. Global fitting efforts which impose unitarity via constrained fits of current experimental and theoretical results start with all these goals. But very different approaches and considerations of inputs result in quite different conclusions.

Partial results of two of the more extensive global fitting efforts, those of Hocker *et al.* ⁸⁾ and Ciuchini *et al.*, ²⁸⁾ are shown graphically in Figs. 8 and 9. Both fits use information available after the summer 2000 conference season. While the final fit contours both center in the same general $(\bar{\rho}, \bar{\eta})$ region, two significant differences between their analyses stand out: a Bayesian vs. frequentist statistical approach to the problem, and the treatment of theoretical

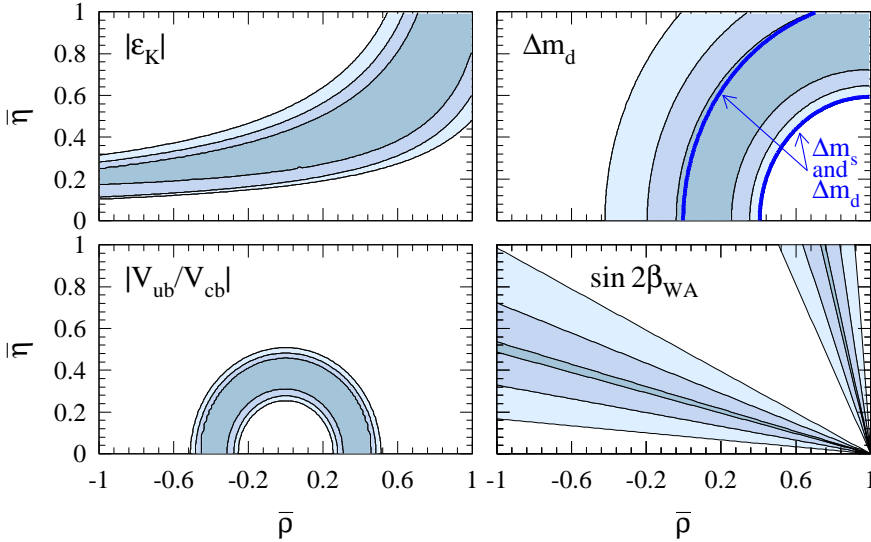


Figure 7: Frequentist CL's δ) for different constraints in the $(\bar{\rho}, \bar{\eta})$ plane. The bands contain regions of $\geq 90\%$, $\geq 32\%$, and $\geq 5\%$, respectively. [from ref. 8]

errors. The *aggressive Bayesians* contend ^{28, 29)} that LQCD theoretical calculations are sufficiently mature to ascribe probabilistic meanings to central values and uncertainties no different from experimental systematics; moreover they maintain that a Bayesian procedure is entirely justified and results in a clearer interpretation of fit results. The counter-argument ^{8, 30)} emphasizes that many of the theoretical inputs are not well-known and therefore cannot be treated as having statistical or Gaussian errors. Furthermore, the *conservative frequentist* viewpoint continues, the more difficult theoretical calculations should be assigned an *allowed range, without any preferred central value*. For such quantities the theoretical values *should not contribute* to the χ^2 , ranging freely over the entire allowed range for any fixed point in fitting-parameter space. Also pointed out is a pernicious and subtle effect of Bayesian combination of as few as three variables specified to have no preferred central value within a range: the Bayesian treatment can easily give a fallaciously narrowed and therefore misleading combined fit. The latter effect occurs even using flat (rather than Gaussian) probability density functions. The importance of these differences in approach will increase as more accurate data become available;

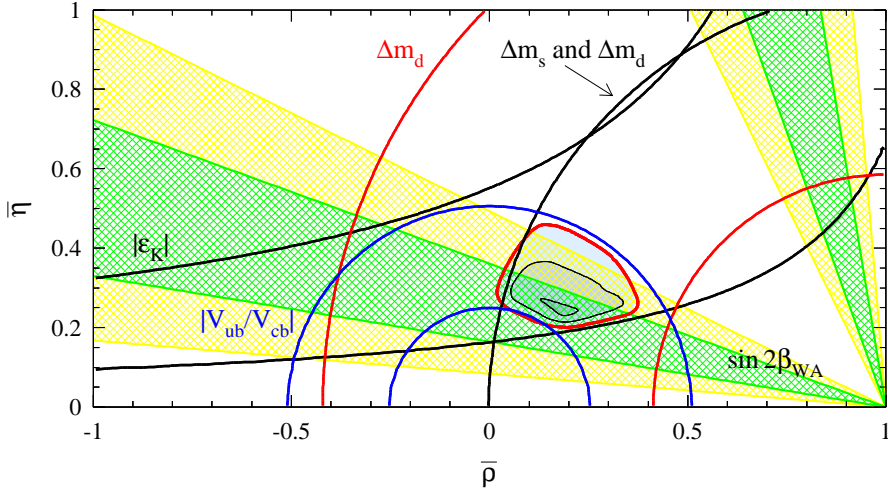


Figure 8: *Frequentist CL's*⁸⁾ for in the $\bar{\rho}, \bar{\eta}$ plane for the global fit of Hocker, et al.⁸⁾ The contours contain regions of $\geq 90\%$, $\geq 32\%$, and $\geq 5\%$, respectively; $\geq 5\%$ levels are shown for individual constraints. [from ref. 8]

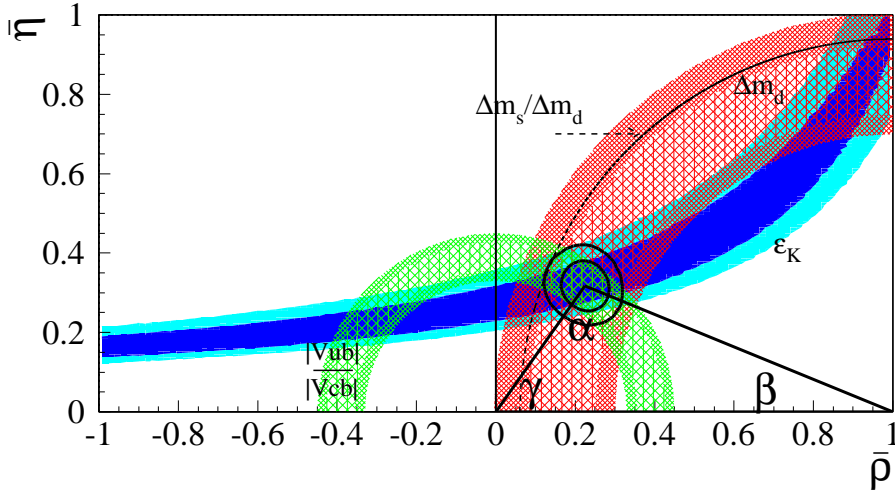


Figure 9: *Confidence levels* for in the $\bar{\rho}, \bar{\eta}$ plane for the global fit of Ciuchini, et al.²⁸⁾ Regions of $\geq 68\%$ and 95% confidence level are shown by the contours (for the fit) and shaded areas (for the individual constraints). [from ref. 28]

it is conceivable that in addition to contrasting “conservative” vs. “aggressive” errors, they could come to conflicting conclusions on consistency with unitarity. These are not small considerations, and deserve further attention.

7 The Role of CLEO-c

Progress in resolving CKM metrology and unitarity consistency is limited by a dearth of robust, accurate, and reliable non-perturbative QCD predictions. This point is made graphically in Fig. 10, which shows the dramatic effect on contours in the (ρ, η) plane of arbitrarily shrinking contributions from theoretical errors to the 2%-level. New results from the B -factories will only serve to highlight the problem by increasing the disparity between experimental and theoretical precision. LQCD is poised to provide the requisite relief in the coming years (Section 3). However, in order to have any credibility, more accurate predictions must be confronted with equally accurate measurements. With only a handful of fundamental adjustable parameters (quark masses and the strong coupling constant), LQCD must be challenged to account for as large a set of observations within its domain as possible. At percent-level precision, there is now a paucity of the necessary experimental cross-checks available.

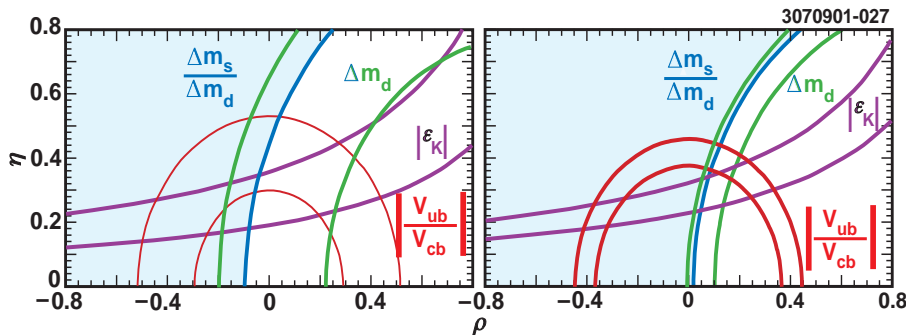


Figure 10: 90% confidence level contours in the (ρ, η) -plane from four measured observables, including current theoretical and experimental errors (left) and after shrinking the relative theoretical uncertainties to the 2%-level.

The CESR-c/CLEO-c ³¹⁾ program is designed to fill this experimental void on an ideal time-scale. The plan calls for e^+e^- datasets of unprecedented size in the tau-charm and Υ energy regimes with a modern, well-seasoned detector over a five year period. Only modest enhancements to the CESR collider,

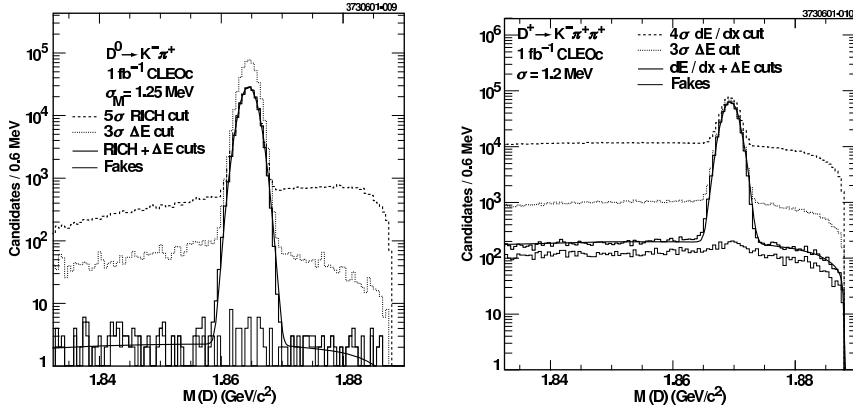


Figure 11: Reconstructed $K^-\pi^+$ and $K^-\pi^+\pi^+$ D -candidate mass distributions for CLEO-c Monte Carlo events generated at $D\bar{D}$ threshold.

in the form of new superconducting wiggler magnets, are necessary to run in the center-of-mass energy range from $\sqrt{s}=3-11$ GeV with peak luminosity scaling as $\sim s$, $\mathcal{L} \approx 0.15 - 1.2 \times 10^{33} \text{ cm}^{-2} \text{ sec}^{-1}$. Few changes to the CLEO III detector, infrastructure, and analysis tools are required; CLEO-c will easily be the most capable detector to have run in this energy range. Datasets of 10^9 events at the J/ψ , 3 fb^{-1} at each of $D\bar{D}$ and $D_s\bar{D}_s$ thresholds, and 1 fb^{-1} at each of $\Upsilon(1S)$, $\Upsilon(2S)$, and $\Upsilon(3S)$ resonances will provide precise benchmark measurements with which to confront emerging LQCD calculations.

The decay constants for D and D_s can be measured accurately at pair-production thresholds by flavor-tagging with a fully-reconstructed known decay and looking for the $\mu\nu$ (and $\tau\nu$ for D_s) of the appropriate charge and kinematics, thereby measuring the branching fraction. The cleanliness of single-tag D and D_s samples is shown in Fig. 11 and 12. Fig. 13 shows missing-mass-squared distributions for tagged $D, D_s \rightarrow \mu\nu$ samples from 1 fb^{-1} at each threshold; signal events are copious and well-separated from dangerous backgrounds, projecting to $\leq 4\%$ uncertainty these branching fractions. Combined with the corresponding lifetime errors of $\leq 2\%$ and $|V_{cj}|$ errors of $\leq 1\%$ obtained from unitarity, relative uncertainties of $\sim 2\%$ are expected for both f_D and f_{D_s} .

Another strength of CLEO-c is its ability to isolate and measure semi-leptonic decays cleanly, as shown for $D \rightarrow \pi l\nu$ in Fig. 14. Such measurements

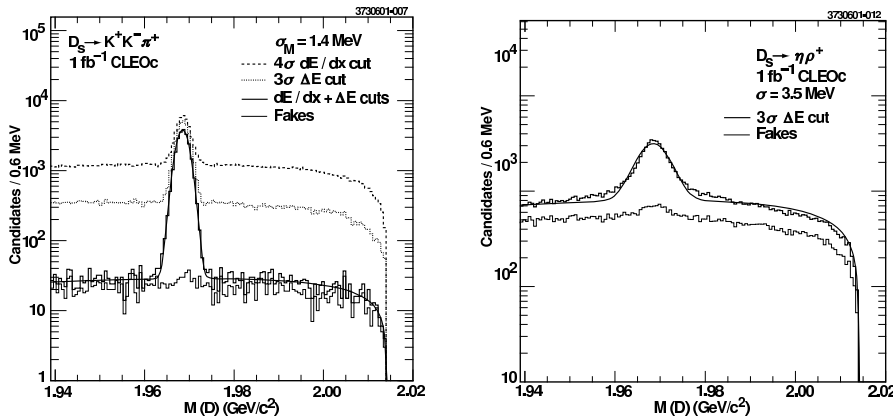


Figure 12: Reconstructed $K^+K^-\pi^+$ and $\eta\rho^+$ D_s -candidate mass distributions for CLEO-c Monte Carlo events generated at $D_s\bar{D}_s$ threshold.

allow the determination of form-factor *shapes* for comparison with theory, and $|V_{cj}|$ using the measured branching fractions along with normalization from theory. These shapes and normalizations can be cross-checked with a large variety of exclusive semi-leptonic decay modes, with uncertainties expected in the few percent level. The ratio $|V_{cd}|/|V_{cs}|$, a more straightforward test for theory, will have experimental uncertainties in the 1-5% range.

A second vexing issue for heavy flavor physics is the increasing importance of having accurate D branching fractions, which are beginning to limit corresponding B -physics results. CLEO-c can address this issue as well, by measuring the rate of double- to single-tags for the desired modes. Once again, threshold measurements are seen to be extremely clean and accurate. Branching fractions will be measured to $\sim 1\%$ or better for $D^0 \rightarrow K^-\pi^+$ and $D^+ \rightarrow K^-\pi^+\pi^+$ for D 's and $\sim 2\%$ for $D_s \rightarrow \phi\pi$; correspondingly large improvements over current uncertainties are expected for other modes as well.

A second crucial part of the CLEO-c/CESR-c program is to spend time studying the charmonium and bottomonium states, where several QCD prizes await. Probing radiative J/ψ decays for the on-again, off-again $f_J(2220)$ should prove decisively whether it exists ¹⁾ and, if so, its status as $q\bar{q}$, glueball, or hybrid. Evidence of the $f_J(2220)$ is conflicting, ³²⁾ but has been reported in

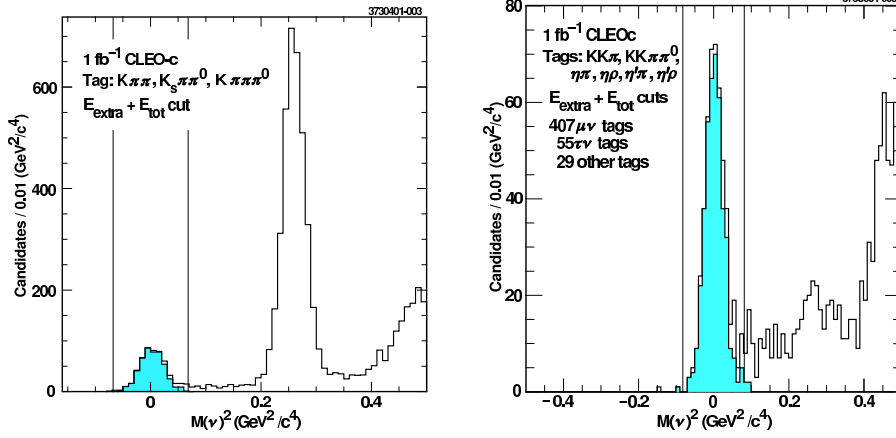


Figure 13: The missing-mass-squared distribution in tagged $D \rightarrow \mu\nu$ (left) and $D_s \rightarrow \mu\nu$ (right) events from CLEO-c Monte Carlo generated at $D\bar{D}$ and $D_s\bar{D}_s$ thresholds, respectively. The shaded areas show correctly tagged candidates. The unshaded peak in the D plot corresponds to $D \rightarrow K_L^0\mu\nu$ background.

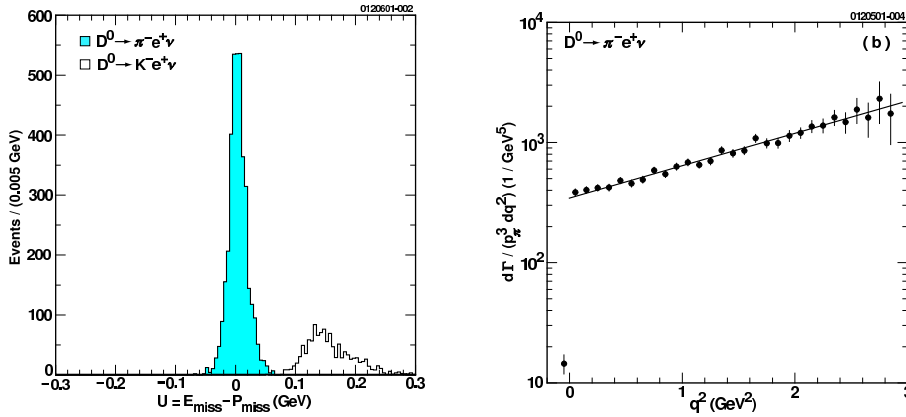


Figure 14: From CLEO-c Monte Carlo generated at $D\bar{D}$ threshold, distributions for tagged $D^0 \rightarrow \pi^- e^+ \nu$ candidates, in a missing-mass variable, shaded region being signal and unshaded misidentified $D^0 \rightarrow K^- e^+ \nu$ background; and in q^2 with the overlayed fit for the form-factor.

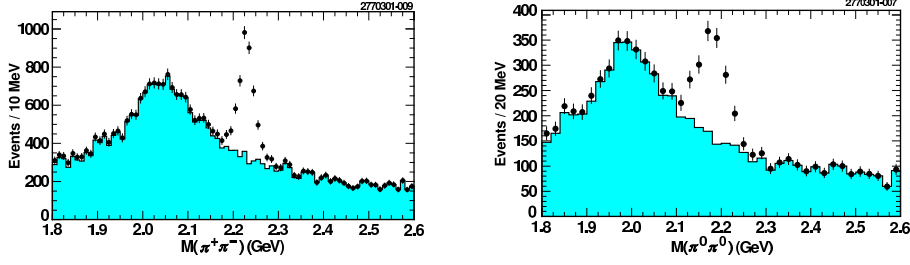


Figure 15: *Two-particle mass distributions for $J/\psi \rightarrow \gamma\pi\pi$ candidates in CLEO-c Monte Carlo generated with $f_J(2220)$ at the BES branching ratios $\mathcal{B}(J/\psi \rightarrow \gamma f_J) \times \mathcal{B}(f_J \rightarrow \pi\pi) \sim 5 \times 10^{-5}$. Each plot corresponds to a sample of $\sim 150M$ J/ψ decays and has $\mathcal{B}(J/\psi \rightarrow \gamma f_4(2050)) = 2.7 \times 10^{-3}$, $\mathcal{B}(f_4(2050) \rightarrow \pi\pi) = 0.17$.*

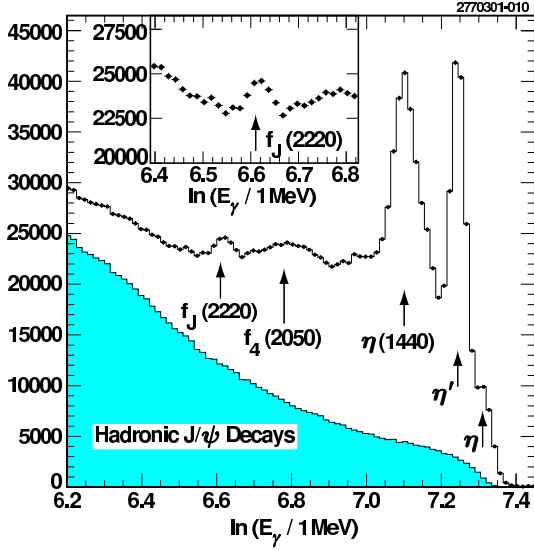


Figure 16: *Inclusive photon spectrum in CLEO-c Monte Carlo of $60M$ J/ψ decays, showing sensitivity a $f_J(2220)$ signal with $\mathcal{B}(J/\psi \rightarrow \gamma f_J(2220)) = 8 \times 10^{-4}$ in relation to backgrounds with $\mathcal{B}(J/\psi \rightarrow \gamma f_4(2050)) = 2.7 \times 10^{-3}$ and $\mathcal{B}(J/\psi \rightarrow \gamma \eta(1440)) = 4.5 \times 10^{-3}$.*

$K\bar{K}$, $\pi^+\pi^-$, $\pi^0\pi^0$, and $p\bar{p}$ final states. Fig. 15 shows CLEO-c’s sensitivity for two of these modes in exclusive $J/\psi \rightarrow \gamma f_J(2220)$ when produced at the observed BES branching fractions in a small fraction of the projected CLEO-c dataset of 10^9 J/ψ ’s. If it exists anywhere near this level, it will be seen and a partial-wave analysis will measure its quantum numbers J^{PC} . The inclusive photon spectrum, as shown in Fig. 16, will also prove to be a powerful tool in discovery or confirmation of any narrow resonance produced in radiative J/ψ decays. If the $f_J(2220)$ is truly a glueball, it should not be seen in the ~ 20 fb^{-1} of CLEO II and CLEO III data (or Belle or BaBar’s either) as a product of two-photon collisions; CLEO has already set a limit ³³⁾ based on 4.8 fb^{-1} .

Other interesting quarkonia physics topics which will provide more much-needed grist for the LQCD mill, include discovery and mass-measurement of the η_b (ground state 1S_0 of $b\bar{b}$), h_b (1P_1), glueballs in glue-rich radiative Υ decays, glue-quark hybrid states, scalar resonances with or without glue content in radiative J/ψ decays, and many, many more.

One might well ask how the above capabilities stack up against that expected from BES, or against B -factories with ~ 400 fb^{-1} . While it is always risky to bet what someone else is not capable of, charm physics at the $\Upsilon(4S)$ faces some obstacles that improve only slowly or not at all with more data. Prime among barriers is the absence of the kinematic constraints available at threshold. However, extrapolating from previous CLEO efforts, keeping such obstacles and potential ways around them in mind, yields optimistically three times larger errors on charm decay constants and branching fractions. If these estimates prove to instead be pessimistic, it will still be true that $\Upsilon(4S)$ charm analyses will be systematics-limited in a way that is complementary to CLEO-c. The other competition targeting tau-charm physics is BES II at the BEPC storage ring in Beijing. Currently BEPC operates at more than an order of magnitude lower luminosity than that projected for CESR-c, and the proposed machine and detector upgrades to “factory” levels could be completed by 2005 at the earliest. CLEO-c plays a unique and crucial role in the years ahead.

8 Outlook

The continuing productive interplay among accelerator development, theoretical insight, and experimental technique has brought CKM physics to the threshold of a major transition, one that is qualitative as well as a quantitative. The

B -factories are operating beyond expectations, promising a rich array of new measurements. Foremost among those would be observation of CP violation in B -decays, which can happen with data already in-hand, assuming Nature cooperates. The fortuitously-timed maturation of LQCD along with a reality-grounding CLEO-c experimental program should provide crucial breakthroughs in unraveling the effects of strong interactions. The approach to *precision* CKM physics on both experimental and theoretical fronts is underway.

9 Acknowledgments

Our hosts for *Physics in Collision 2001* and its international and local organizing committees are to be congratulated for organizing a productive and stimulating conference at Seoul National University. The patient assistance of my CLEO colleagues was essential in the preparation of this presentation, and greatly appreciated.

References

1. D.E. Groom *et al.*, *Eur. Phys. J.* **C15**, 1 (2000).
2. SLAC-R-504, *The BaBar Physics Book* (ed. P.F. Harrison and H.R. Quinn, October, 1998).
3. A.J. Buras and R. Fleischer, *Heavy Flavors II* (ed. A.J. Buras and M. Lindner, World Scientific, Singapore, 1997) [hep-ph/9704376].
4. N. Cabibbo, *Phys. Rev. Lett.* **10** (1963) 531.
5. M. Kobayashi and T. Maskawa, *Prog. Theor. Phys.* **49** (1973) 652.
6. L. Wolfenstein, *Phys. Rev. Lett.* **51** (1983) 1945.
7. A.J. Buras, M.E. Lautenbacher and G. Ostermaier, *Phys. Rev. D* **50** (1994) 3433.
8. A. Hocker, *et al.*, *Eur. Phys. J.* **C21** (2001) 225 [hep-ph/0104062].
9. J.P. Silva and L. Wolfenstein, *Phys. Rev. D* **55** 1997, 5331 [hep-ph/9610208]; R. Aleksan, B. Kaiser, and D. London, *Phys. Rev. Lett.* **73** (1994) 18 [hep-ph/9403341]; I.I. Bigi and A.I. Sanda, [hep-ph/9909479].

10. G.P. Lepage and P.B. Mackenzie, *Phys. Rev. D* **48** (1993) 2250.
11. M. Alford *et al.*, *Phys. Lett.* **B361** (1995) 87; M. Luscher *et al.*, *Phys. Lett.* **B478** (1996) 365.
12. I.S. Towner and J.C. Hardy, nucl-th/9809087 (1998); K. Saito and A.W. Thomas, *Phys. Lett.* **B363** (1995) 157.
13. H. Leutwyler and M. Roos, *Z. Phys.* **C25** (1984) 91; R.E. Shrock and L.-L. Wang, *Phys. Rev. Lett.* **41** (1978) 1692.
14. R. Flores-Mendieta, A. García, and G. Sánchez-Colón, *Phys. Rev. D* **54** (1996) 6855; M. Bourquin *et al.*, *Z. Phys.* **C21** (1983) 27.
15. H. Abramowicz *et al.* (CDHS Collab.), *Z. Phys.* **C15** (1982) 19; A.O. Bazarko *et al.* (CCFR Collab.), *Z. Phys.* **C65** (1995) 189 [hep-ex/9406007]; P. Vilain *et al.* (CHARM II Collab.) *Eur. Phys. J.* **C11** (1999) 19.
16. G. Abbiendi *et al.* (OPAL Collab.), *Phys. Lett.* **B490** (2000) 71.
17. D. Abbaneo *et al.* (LEP V_{cb} Working Group), <http://lepvcb.web.cern.ch/LEPVCB/Winter01.html>.
18. B. Barish *et al.* (CLEO Collab.), *Phys. Rev. Lett.* **76** (1996) 1570.
19. D. Abbaneo *et al.* (LEP V_{ub} Working Group), *LEPVUB-01/01*, June 29, 2001; also <http://battagl.home.cern.ch/battagl/vub/vub.html>.
20. J.P. Alexander *et al.* (CLEO Collab.), *Phys. Rev. Lett.* **77** (1996) 5000; B.H. Behrens *et al.* (CLEO Collab.), *Phys. Rev. D* **61** (2000) 052001 [hep-ex/9905056].
21. D. Abbaneo *et al.* (LEP B -Oscillations Working Group), *CERN-EP-2001-50*, June 26, 2001; also http://www.cern.ch/LEPBOSC/combined_results/budapest_2001.
22. A. Roodman, (BaBar); and M. Rozanska, (Belle); in these proceedings.
23. A.K. Leibovich *et al.*, *Phys. Rev. D* **57** (1998) 308 [hep-ph/9705467].

24. I.I. Bigi, M. Shiffman, and N. Uralsev, *Ann. Rev. Nuc. Part. Sci.* **47** (1997) 591 [hep-ph/9703290].
25. D. Cronin-Hennessy *et al.* (CLEO Collab.), *CLNS/01-1752* (2001) [hep-ex/0108033]; S. Chen *et al.* (CLEO Collab.), *CLNS/01-1751* (2001) [hep-ex/0108032].
26. A. Falk, M. Luke, and M. Savage, *Phys. Rev. D* **53** (1996) 2491 [hep-ph/9507284]; *ibid.* **53** (1996) 6316 [hep-ph/9511454]; M. Gremm and A. Kapustin, *Phys. Rev. D* **55** (1997) 6924 [hep-ph/9603448]; M. Voloshin, *Phys. Rev. D* **51** (1995) 4934 [hep-ph/9411296].
27. N. Isgur, *Phys. Lett.* **B 448** (1999) 111 [hep-ph/9811377]; I.I. Bigi, hep-ph/0009021.
28. M. Ciuchini *et al.*, *J. H. E. P.* *0107* (2001) 13 [hep-ph/0012308].
29. A. Stocchi, in *Proceedings of Beauty 2000, Kibbutz Maagan, Israel, September, 2000* (ed. S. Erhan, Y. Rozen, and P. E. Schlein); *Nucl. Instrum. Meth.* **A462** (2001) 318 [hep-ph/0012215].
30. S. Stone, in *Beauty 2000*, *Nucl. Instrum. Meth.* **A462** (2001) 323 [hep-ph/0012162]; M. Artuso, in *Beauty 2000*, *Nucl. Instrum. Meth.* **A462** (2001) 307 [hep-ph/0012172]; J.L. Rosner, in *Beauty 2000*, *Nucl. Instrum. Meth.* **A462** (2001) 304 [hep-ph/0011184]; A.F. Falk, in *Proceedings of the XIX International Symposium on Lepton and Photon Interactions at High Energies*; *Int. J. Mod. Phys.* **A15S1** (2000) [hep-ph/9908520].
31. R. Briere *et al.* (CESR-c/CLEO-c Taskforces and CLEO-c Collab.), *CLEO-c and CESR-c: A New Frontier of Weak and Strong Interactions*, *CLNS-01/1742* (2001).
32. J.Z. Bai *et al.* (BES Collab.) *Phys. Rev. Lett.* **76** (1996) 3502; *ibid.* **81** (1998) 1179; R.M. Baltrusaitis *et al.* (MARK III Collab.) *Phys. Rev. Lett.* **56** (1986) 107; C. Evangelista *et al.* *Phys. Rev. D* **56** (1997) 3803 [hep-ex/9707041].
33. M.S. Alam *et al.* (CLEO Collab.) *Phys. Rev. Lett.* **81** (1998) 3328 [hep-ex/9805033].